Zero Velocity Detector for Foot-mounted Inertial Navigation System Assisted by a Dynamic Vision Sensor

C.-S. Jao[1], K. Stewart[2], J. Conradt[3], E. Neftci[2], A. M. Shkel[1]

[1] University of California, Irvine, MicroSystems Lab
27 E Peltason Drive, Room 2115
Irvine, CA 92617
USA

[2] University of California, Irvine, Neuromorphic Machine Intelligence Lab
234 Pereira Drive, Room 2308
Irvine, CA 92697
USA

[3] KTH Royal Institute of Technology, Division of Computational Science and Technology,
Lindstedtsvägen 5, Room 4418
Stockholm
Sweden

Inertial Sensors and Systems 2020
Braunschweig, Germany

978-1-7281-6848-7/20/$31.00©2020 IEEE

Abstract

In this paper, we proposed a novel zero velocity detector, the Dynamic-Vision-Sensor (DVS)-aided Stance Phase Optimal dEtection (SHOE) detector, for Zero-velocity-UPdaTe (ZUPT)-aided Inertial Navigation Systems (INS) augmented by a foot-mounted event-based camera DVS128. We observed that the firing rate of the DVS consistently increased during the swing phase and decreased during the stance phase in indoor walking experiments. We experimentally determined that the optimal placement configuration for zero-velocity detection is to mount the DVS next to an Inertial Measurement Unit (IMU) and face the sensor outward. The DVS-SHOE detector was derived in a General Likelihood Ratio Test (GLRT) framework, combining statistics of the conventional SHOE detector and the DVS firing rate. This paper used two methods to evaluate the proposed DVS-SHOE detector. First, we compared the detection performances of the SHOE detector and the DVS-SHOE detector. The experimental results showed that the DVS-SHOE detector achieved a lower false alarm rate than the SHOE detector. Second, we compared the navigation performance of the ZUPT-aided INS using the SHOE detector and the DVS detector. The experimental results showed that the Circular Error Probable (CEP) of the case using DVS-SHOE was reduced by around $25\ \%$ from $1.2\ m$ to $0.9\ m$, as compared to the case of the SHOE detector.

1. Introduction

Pedestrian Dead Reckoning (PDR) systems, or self-contained pedestrian Inertial Navigation Systems (INS), are necessary for localization in environments where the signals of Global Navigation Satellite Systems (GNSS) are degraded or unavailable [1]. In the GNSS-degraded environments, alternative localization techniques include 1) radio navigation systems utilizing signals from Wireless Local Area Network (WLAN) [2], Bluetooth [3], Long-Term Evolution (LTE) [4], and Ultra-Wide Band(UWB) [5] and 2) vision-based navigation systems that utilizes computer vision algorithms to estimate camera positions based on visual features detected in the surrounding environments [6, 7]. However, in some scenarios, the assumptions about availability of Radio-Frequency (RF) infrastructure and validity of images for visual feature detection might not be realistic. Thus, self-contained pedestrian INS are the only remaining options.

Due to the successful development of Micro-Electro-Mechanical-System (MEMS), small-size and low-cost Inertial Measurement Units (IMUs) have become available, and the availability has enabled pedestrian INS. However, the positions estimated by an INS have high drift because the INS performs positioning by dead reckoning utilizing noisy IMU

measurements that are corrupted by unknown time-varying biases [8]. For pedestrian navigation, the Zero velocity UPdaTe (ZUPT) algorithm, can enhance the navigation accuracy of an INS employing foot-mounted IMUs. The ZUPT-aided INS calibrates the IMU measurements and zeros out the residual velocity of the INS during the stance phase in a gait cycle [9]-[13]. The standalone ZUPT-aided INS has demonstrated the capability of achieving an accuracy of 1 meter after traveling on the order of 100 meters, with industrial-grade inertial sensors [14]. The accuracy of the ZUPT-aided INS could be further improved by fusing IMU measurements, ZUPT algorithm, and measurements of other non-inertial sensors, such as barometers, ultrasonic sensors, magnetometers, and cameras [15]-[20]. However, the navigation error of ZUPT-based INS heavily depends on the performance of stance phase detection. For example, a standalone ZUPT-aided INS that employs an accurate stance phase detector could have a better navigation performance than a ZUPT/barometer-aided INS that uses an inaccurate stance phase detector.

In early developments of the ZUPT algorithm for pedestrian navigation, stance phase detection, or zero velocity detection, was often achieved by comparing a fixed threshold with statistics of likelihood computed from accelerometers' and gyroscopes' measurements [21]. One of the frequently used detector is the Stance Hypothesis Optimal dEtection (SHOE) detector. The statistics of the SHOE detector directly relates to stability of the foot, and its detection mechanism is based on an observation that the foot is more stable in the stance phase than in the swing phase. As a result, if the statistics is higher than the defined threshold, the SHOE detector determines the swing phase. Otherwise, the detector indicates the stance phase.

The statistics of the SHOE detector, however, has an undesirable property. Figure 1 presents an example of statistics of the SHOE detector of one gait cycle in an indoor walking experiment. In the second stage of the swing phase, the statistics of the SHOE detector decreased when compared to the first and the second stages. The decrease was due to the fact that the foot is more stable when traveling in the air than when taking off or landing. False alarms of zero velocity detection, which is defined as the case that a detector determines as a stance phase when the foot is in the swing phase, often occur during the period when the foot is in the air. For example, if we used the threshold, indicated by the red line in Figure 1, then a false alarm would be triggered. Notice that although we can lower the threshold value to eliminate the false alarm, the lower value does not necessarily lead to an improved overall navigation result.

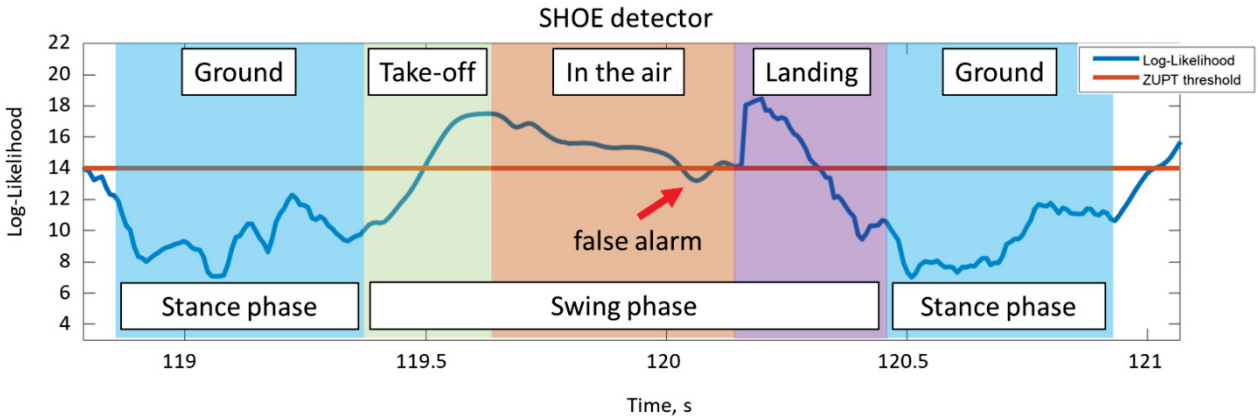

Figure 1. An example of the SHOE statistics in one gait cycle. The gait cycle is split into two stance phases and a swing phase. The swing phase can be further divided into three stages. In the first stage, the foot takes off the ground. In the second stage, the foot travels in the air. In the third stage, the foot lands on the ground.

Previous work on improvement of the detection performance of zero velocity detection can be categorized into two groups. The first group uses thresholds that adaptively vary during different activities, such as walking, running, and climbing. The adaptive approaches include classifications based on machine learning, Long Short-Term Memory (LSTM) neural network, Hidden Markov Model (HMM), the posterior odds, the temporal variance of the accelerometer, and the maximum shock of an IMU [22]-[32]. The methods presented in the first group usually involve large training datasets and multiple heuristic parameter tuning. Thus, it is not ideal for real-time implementation.

The second group of approaches includes measurements of other non-inertial sensing modalities in the computation of likelihood statistics. Sensor modalities including magnetometers [33], electromyography (EMG) [34], shoe-embedded pressure sensors [35], and downward-facing Radio Frequency (RF) sensors [36]-[38] have been explored for this purpose. However, these approaches for enhancing zero-velocity detection also have limitations and constraints. The systems with EMG sensors are physically too complex. The systems integrated with shoe-mounted pressure sensors or downward-facing ranging sensors are only effective when users step on the ground and would fail for other pedestrian activities, such as climbing on ladders. Therefore, other sensing modalities that could benefit zero-velocity detection without the requirement of shoe contacting the ground are necessary to investigate. In this paper, we utilize a Dynamic Vision Sensors (DVS) to explore how the sensor can help to reduce the false alarm rate of the SHOE detector and improve the detection performance.

DVS, or Event-based cameras, work differently from a traditional CMOS camera in a way that a DVS asynchronously detects light intensity changes, called events [39]. Some previous work has been conducted to apply the DVS to the field of navigation [40]-[42]. The DVS has a high dynamic range, high temporal resolution, low power consumption, and reduced motion blur [43], making it an intriguing alternative for efficient event detection in foot-mounted INS navigation. Since DVS detects light intensity changes, no event would be generated in an ideal case if no object is moving inside its Field Of View (FOV). This idea can be extended to detect whether a DVS is stationary. Under the assumption that the background inside the FOV is static, a DVS has a property that no event would be produced when DVS is static, and a large number of events would be generated when the DVS is moving. In this paper, we utilize this property of a DVS to assist the SHOE detector.

We propose an event-based camera-assisted zero velocity detector for foot-mounted INS. The proposed detector achieves zero-velocity detection by comparing a threshold with its statistics, computed using the firing rate, defined as the total number of events generated during a period, of the event-based camera and the statistics from the SHOE detector. The proposed detector is shown to reduce the rate of false alarms of zero velocity detections and to increase the accuracy of pedestrian navigation. This paper makes the following contributions:

1) it presents hardware design of a foot-mounted INS integrated with a DVS,
2) it analyzes the properties of the DVS firing rate during indoor navigation experiments,
3) it derives the event-based camera-aided zero velocity detector in a Generalized Likelihood Ratio Test (GLRT) framework,
4) it evaluates the proposed detector in terms of detection rate, false alarm rate, and navigation error,
5) it experimentally demonstrates the validity of the proposed detector.

2. Foot-mounted Dynamic Vision Sensor

2.1. The Lab-On-Shoe platform integrated with a DVS128

To understand the characteristics of measurements obtained from a foot-mounted DVS and investigate its effect when aiding foot-mounted IMU for pedestrian inertial navigation,

we combined the Lab-On-Shoe platform with a mini-eDVS system, shown in Figure 2. The Lab-On-Shoe was previously developed by UCI MicroSystems Lab for evaluating navigation performance of foot-mounted IMUs when aided by other non-inertial sensors, such as barometers, ultrasonic sensors, and cameras [44]. The mini-eDVS system

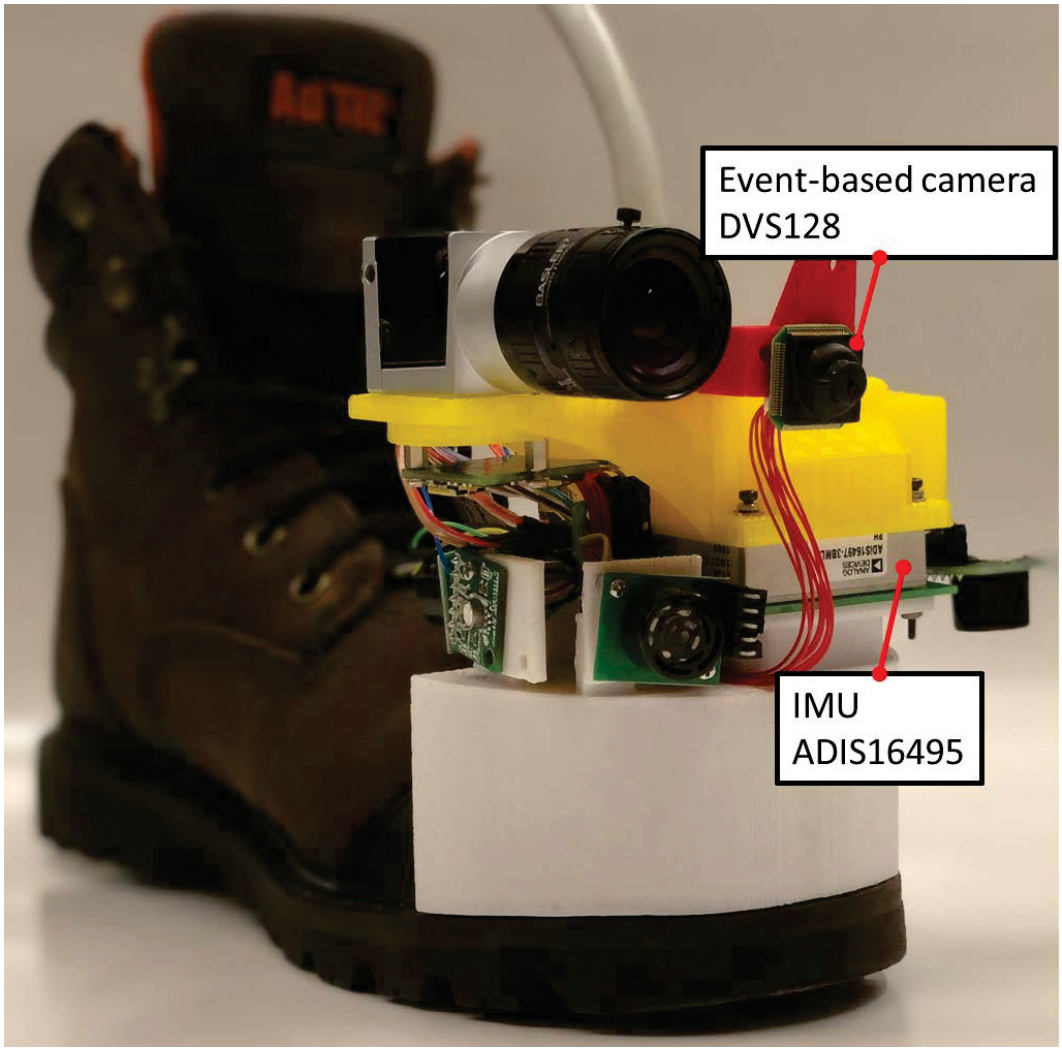

Figure 2. The Lab-On-Shoe platform integrated with DVS128. The Lab-On-Shoe platform is equipped with an IMU, three ultrasonic sensors, an barometer, an CMOS camera, and a DVS. This paper only uses the DVS and the IMU.

contains an event-based camera DVS128 and a micro-controller [40]. The detail description of the event-based camera DVS128 can be found in [39]. In this paper, the IMU sampling rate was set to $120\ Hz$. The DVS firing rate was obtained by calculating the number of events generated in a period of $0.0083\ s$.

2.2. Measurements of foot-mounted DVS

A DVS asynchronously detects light intensity changes, called events. A positive light intensity change is represented as a positive event, and a negative change is a negative

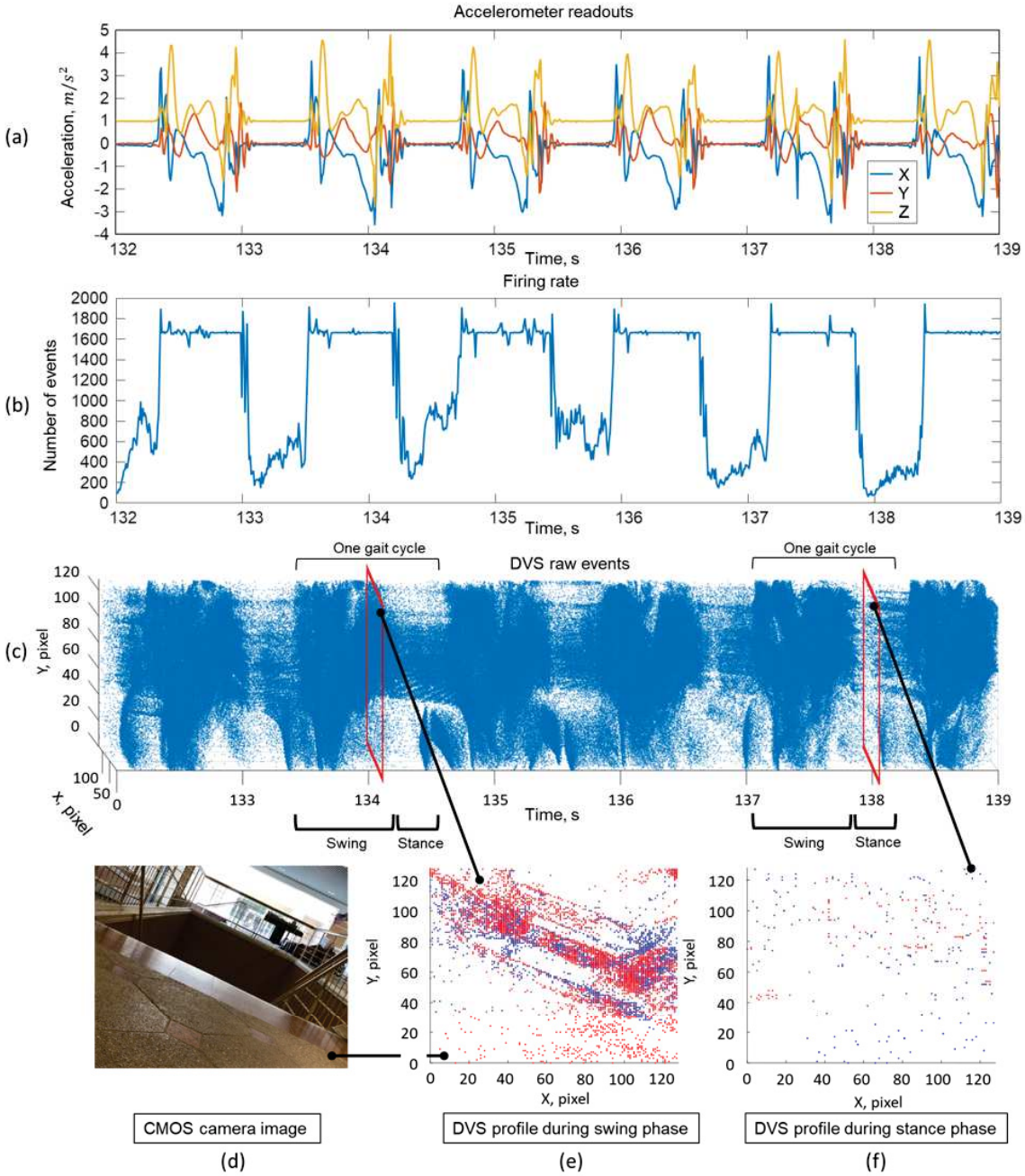

Figure 3. (a) The accelerometer readouts in an indoor walking experiment. (b) The corresponding DVS firing rate in the same experiment. (c) An example of DVS events collected in the same experiment. (d) A group of events collected during a swing phase in the experiment. (e) A CMOS image of the scene generating DVS events during the swing phase. (f) A group of events collected during a stance phase in the experiment.

event. In this paper, we do not distinguish the two types of events as they are both generated by light intensity changes. One scenario that events are produced is when a scene observed is moving relatively to the DVS. In the case of a shoe-mounted DVS in a walking experiment, a large number of events are produced when the shoe is moving, and fewer events present when the shoe is stationary. An example of DVS events generated in an indoor walking experiment is shown in Figure 3(c). Each of the blue particles in Figure

3(c) is an event. For visualization, we collected the events generated in a $0.0083\ s$ window and displayed the events as an DVS image. Figure 3(e) and (f) illustrate DVS images taken during a swing phase and a stance phase, respectively. The blue and the red particles in Figure 3(e) and (f) represent positive and negative events. We can observe that the number of events generated during the stance phase is distinctively less than the swing phase. Note that even though the shoe-mounted DVS had minimum movement during the stance phase, events exist in Figure 3(f). Those events are considered as noise events.

The firing rate of a DVS is defined as the total number of events triggered within a period. The DVS firing rate of the walking experiment is presented in Figure 3(b). Accelerometer readouts collected in the same walking experiment, shown in Figure 3(a), are used as references to the stance phases and the swing phases. Figure 3(b) illustrates that the firing rate increases during the swing phases and decreases during the stance phases. Thus, the firing rate of a shoe-mounted DVS can be used to assist the SHOE detector, which only relies on IMU measurements.

2.3. Mounting position for DVS to achieve best zero-velocity detection performance

To maximize the assistance that a DVS can provide for zero-velocity detection, we conducted two indoor walking experiments with the Lab-On-Shoe platform integrated with the DVS128 to determine a mounting configuration for the DVS. The two experiments were conducted with the same path and walking speed and different mounting configurations for the DVS. The mounting configuration of the DVS in the first experiment is illustrated in Figure 4(a), where the DVS was mounted next to the IMU and faced outward to surrounding walls. In the second experiment, the DVS was mounted on top of the IMU and faced toward the front. The configuration of the second experiment is shown in Figure 4(b).

Figures 4(c) and (d) illustrate examples of the firing rates collected during the first and the second experiments, respectively. Comparing the firing rates in the swing phase, we can see that the configuration demonstrated in Figure 4(a) led to a consistent DVS firing rate. In contrast, the firing rate collected with the configuration shown in Figure 4(b) fluctuated dramatically. The fluctuation was contributed by the fact that with the configuration in Figure 4(b), there is a period during the swing phase that the FOV of the DVS was facing the ground. The ground in the experiments does not have many visual features. Thus, the number of events that were generated was less when the DVS is facing the ground. An

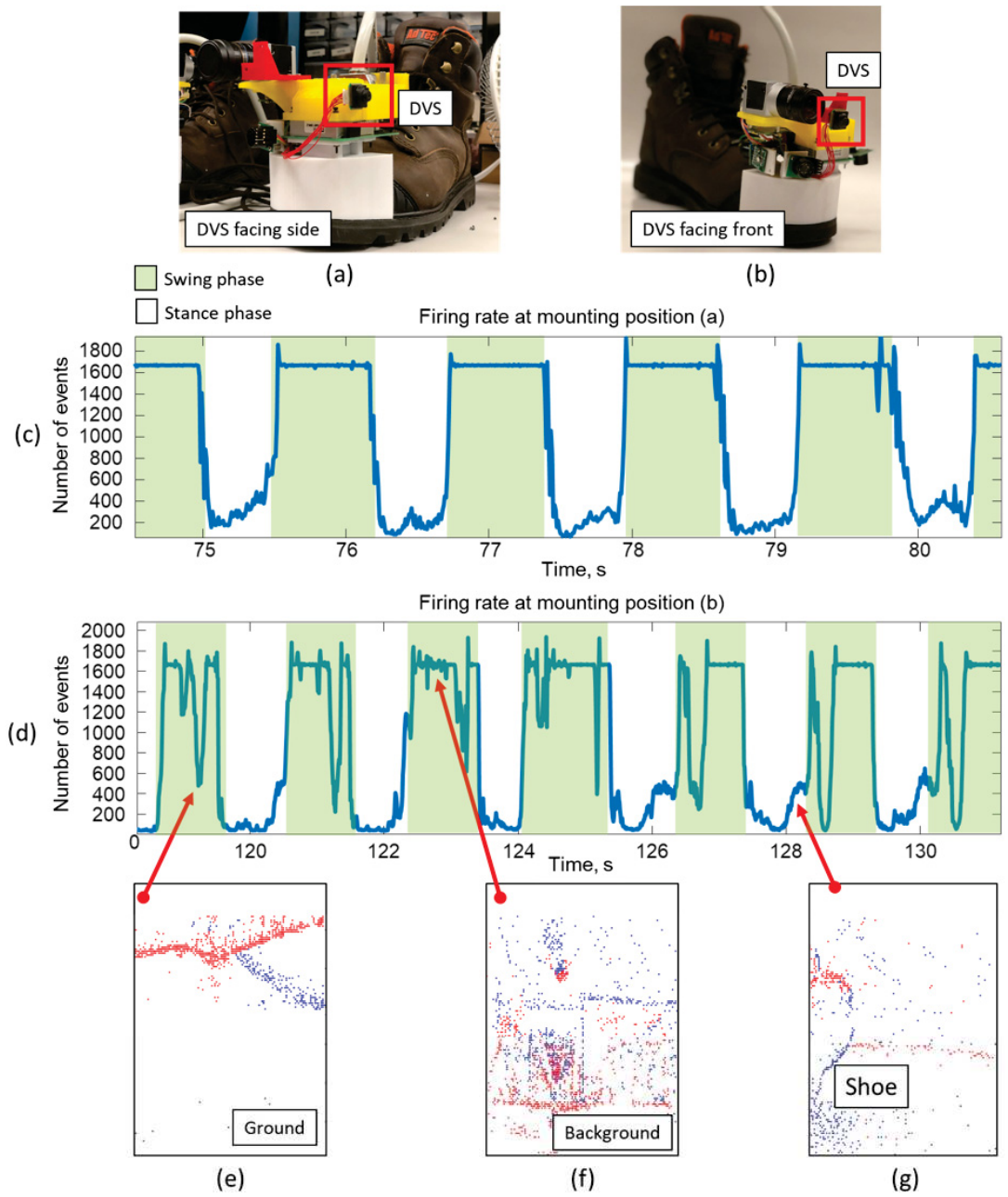

Figure 4. (a) DVS is mounted next to the IMU and faces outward. (b) DVS is mounted next to the IMU and faces outward. (c) Firing rate in an indoor walking experiment with DVS mounting configuration shown in (a). (d) Firing rate in an indoor walking experiment with DVS mounting configuration shown in (b). (e) An example of a DVS image taken when the DVS is facing the ground. (f) An example of a DVS image taken when the DVS is moving and facing forward. (g) An example of a DVS image taken during the stance phase, capturing events generated by the other shoe.

example of events generated when the DVS was facing the ground is shown in Figure 4(e). In this series of experiments, we also found that using the configuration in Figure 4(b) has another drawback. During the stance phase, the other shoe can come inside the FOV of the DVS, generating events that are not beneficial for zero-velocity detection. Figure

4(g) shows an example of the events caused by the other shoe. Since zero-velocity detection is based on comparing a statistics of likelihood with a threshold, one of the desired properties is that the statistics during the stance phase is distinct from that during the swing phase. Thus, to achieve the best performance for zero velocity detection, we conclude that the DVS should be mounted next to the IMU, facing outward.

3. DVS-aided Zero Velocity Detection (DVS-SHOE)

We propose a zero velocity detector that utilizes statistics of the SHOE detector and firing rate of a DVS. We will refer to the proposed detector as the DVS-aided SHOE (DVS-SHOE) detector in the following discussion. The derivation of the DVS-SHOE is similar to the derivation of the SHOE detector presented in [21], which uses the GLRT framework. In the derivation of the DVS-SHOE detector, we augmented the inertial sensors measurements, y_k^α and y_k^ω, with the DVS firing rate, y_k^λ, and the measurement vector y_k can be expressed in the following form:

$$y_k = \begin{bmatrix} y_k^\alpha \\ y_k^\omega \\ y_k^\lambda \end{bmatrix} = \begin{bmatrix} s_k^\alpha \\ s_k^\omega \\ s_k^\lambda \end{bmatrix} + \begin{bmatrix} v_k^\alpha \\ v_k^\omega \\ v_k^\lambda \end{bmatrix} = s_k + v_k,$$

where $s_k^\alpha \in \mathbb{R}^3$ and $s_k^\omega \in \mathbb{R}^3$ denote the IMU-experienced acceleration and angular rate, respectively. $s_k^\lambda \in \mathbb{R}$ denotes the firing rate of the DVS. $v_k^\alpha \in \mathbb{R}^3$, $v_k^\omega \in \mathbb{R}^3$, and $v_k^\lambda \in \mathbb{R}$ represent the measurement noises of the accelerometer, gyroscope, and DVS firing rate, respectively. In our derivation, we assumed that the measurement noises of accelerometers, gyroscopes, and DVS firing rate are independent and identically distributed white Gaussian noises with respective variances σ_α^2, σ_ω^2, and σ_λ^2.

As discussed in [21], the two hypotheses, H_0 and H_1, in zero-velocity detection correspond to the cases of the swing phase and the stance phase, respectively. Under the hypothesis H_1, the accelerometer only experiences the gravitational acceleration; the angular rate experienced by the gyroscope is zero; the DVS firing rate is a constant value λ. For an ideal noise-free DVS, λ is zero. In a practical situation, noise events can be generated even when no object is moving in a DVS field of view, and therefore, λ is non-zero. In our implementation, we experimentally determined $\lambda = 30$. Under the hypothesis H_0, forces from the foot lead to complicated foot motion, so that the accelerometer experiences acceleration exceeding gravity, the gyroscope readouts fluctuate, and the DVS detects

events generated by the foot motion. For the two hypotheses, we assumed the sensor measurements should satisfy the following conditions:

$$H_0: \exists k \in \Omega_n, s_k^{\alpha} \neq g u_n, s_k^{\omega} \neq 0_{3\times1}, s_k^{\lambda} \neq \lambda$$

$$H_1: \forall k \in \Omega_n, s_k^{\alpha} = g u_n, s_k^{\omega} = 0_{3\times1}, s_k^{\lambda} = \lambda$$

where u_n is a 3×1 unit vector, $0_{3\times1}$ is a 3×1 zero vector, g is the gravitational constant, and $\Omega_n = \{l \in N, n \leq l < N-1\}$ is a collection of the sensor measurement indexes at time n with a window of length N.

Following the derivation described in [21], the proposed DVS-SHOE detector chooses H_1 if

$$T_{\lambda}(z_n) = \frac{1}{N}\sum_{k\in\Omega_n}\left(\frac{1}{\sigma_{\alpha}^2}\left\|y_k^{\alpha} - g\frac{\bar{y}_k^{\alpha}}{\|\bar{y}_k^{\alpha}\|}\right\|^2 + \frac{1}{\sigma_{\omega}^2}\|y_k^{\omega}\|^2 + \frac{1}{\sigma_{\lambda}^2}\|y_k^{\lambda} - \lambda\|^2\right) < \gamma',$$

where $z_n = \{y_k\}_{k=n}^{k=N-1}$ and γ' are user-defined thresholds.

4. Experimental Results

To validate the DVS-SHOE detector, we performed a series of indoor close-loop walking experiments with the Lab-On-Shoe platform integrated with the DVS128. The series of experiments included ten nominally identical trials. In each trial, a subject walked over 150 steps for a duration of $160\ m$ in about $120\ s$. The trajectory included a flat surface, a ramp, and stairs. A reference trajectory generated by ZUPT-aided INS with the DVS-SHOE detector is shown in Figure 6(a). We used two methods to evaluate the DVS-SHOE detector. The first method was to study the detection performance in terms of the detection rate and the false alarm rate. The second method was to investigate the navigation results of ZUPT-aided INS with different detectors. Detailed implementation of the ZUPT-aided INS is presented in [11].

4.1. Detector Performance

We first compared the detection performance of the DVS-SHOE detector with the SHOE detector. False alarm rate and detection rate were used as metrics for evaluation. In zero-velocity detection, a false alarm is generated when the shoe is moving, but a stance phase detector indicates a stance phase. A mis-detection is produced when the shoe is on the ground, but the detector determines a swing phase. Figure 5(a) illustrates that using the threshold indicated by the green line in Figure 5(a) for the SHOE detector would lead to a

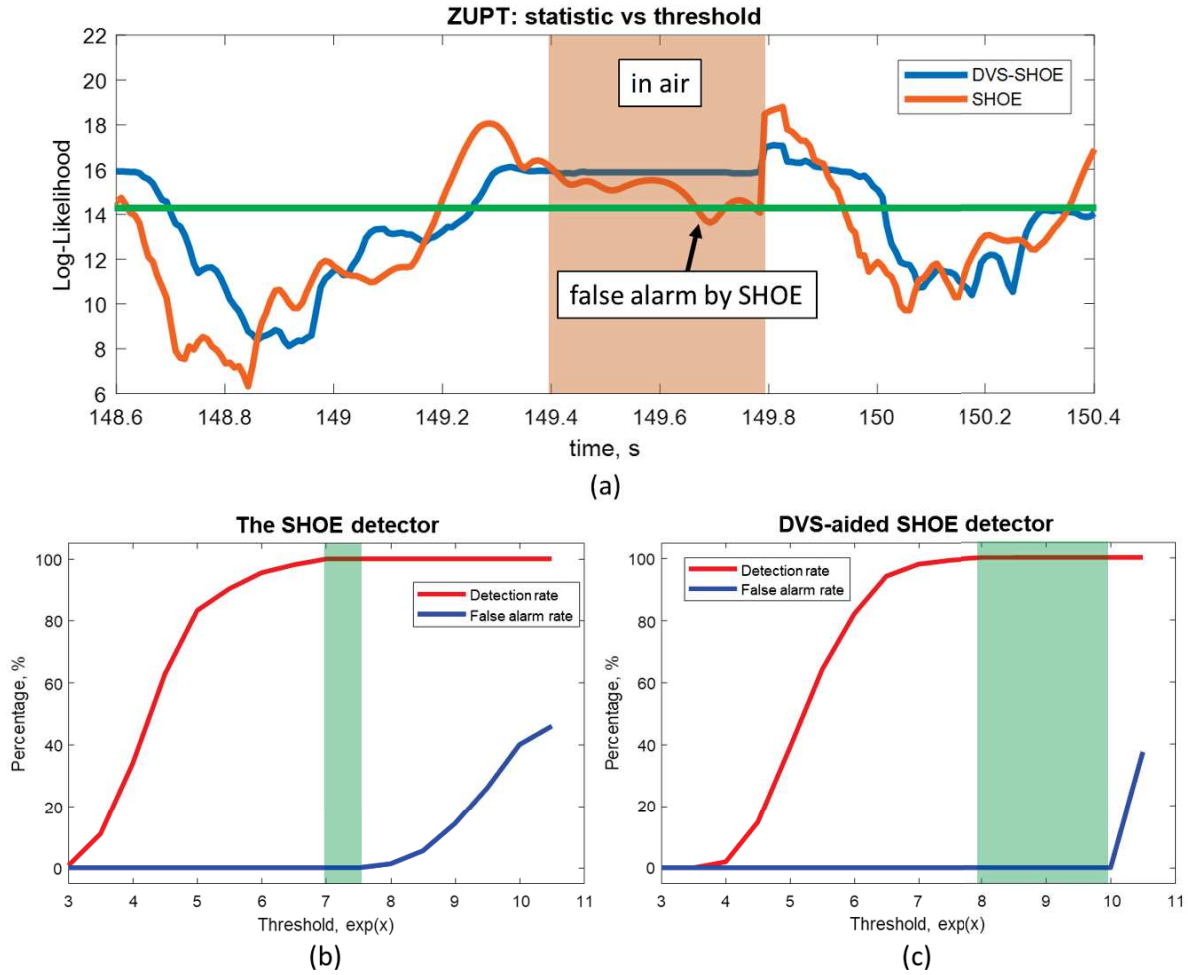

Figure 5. (a) shows an example of SHOE and DVS-SHOE statistics for one gait cycle in the indoor walking experiment. The orange area indicates the stage of shoe traveling in the air during the swing phase. (b) presents the detection performance of the SHOE detector in the indoor walking experiments. The green area indicates the range of thresholds that achieves a near 0% false alarm and 100% detection rate. (c) demonstrates the detection performance of the DVS-SHOE detector in the indoor walking experiments. The green area in (c) is larger than the one shown in (b). The larger green area implies that the DVS-SHOE detector is more robust than the SHOE detector.

false alarm in the walking experiment. The false alarm was eliminated when the statistics of the DVS-SHOE was used. The elimination was due to the fact that during the period when the shoe is traveling in the air, the DVS firing remains consistently on a high level. Thus, the statistics of the DVS-SHOE was kept high during the orange area in Figure 5(a), leading to a reduction of the false alarm.

Figure 5(b) and (c) demonstrate the detection rates of the SHOE detector and the DVS-SHOE detector when different values of thresholds were used. We can observe that the first false alarm for the DVS-aided SHOE detector happened at a much larger threshold value than in the case of the SHOE detector. The green areas in both Figure 5(b) and (c) indicate that when a threshold value is chosen from this range, the detector achieves a

near 0% false alarm rate and a 100% detection rate. In this series of experiments, the green area in Figure 5(e) is larger than Figure 5(d), implying that the DVS-SHOE detector can handle a larger range of thresholds.

4.1. Navigation results

To evaluate the DVS-SHOE detector in a more realistic case, we compared the navigation accuracy of ZUPT-based INS when using the SHOE detector and the DVS-SHOE detector. The navigation accuracy is evaluated with the Circular Error Probable (CEP). The estimated final destinations of the ten sets of experiments and the CEPs are presented in Figure 6(b) and (c). The experimental results showed that the CEP is reduced by around 25%, from $1.2\,m$ to $0.9\,m$, when the DVS-aided SHOE detector is applied. The

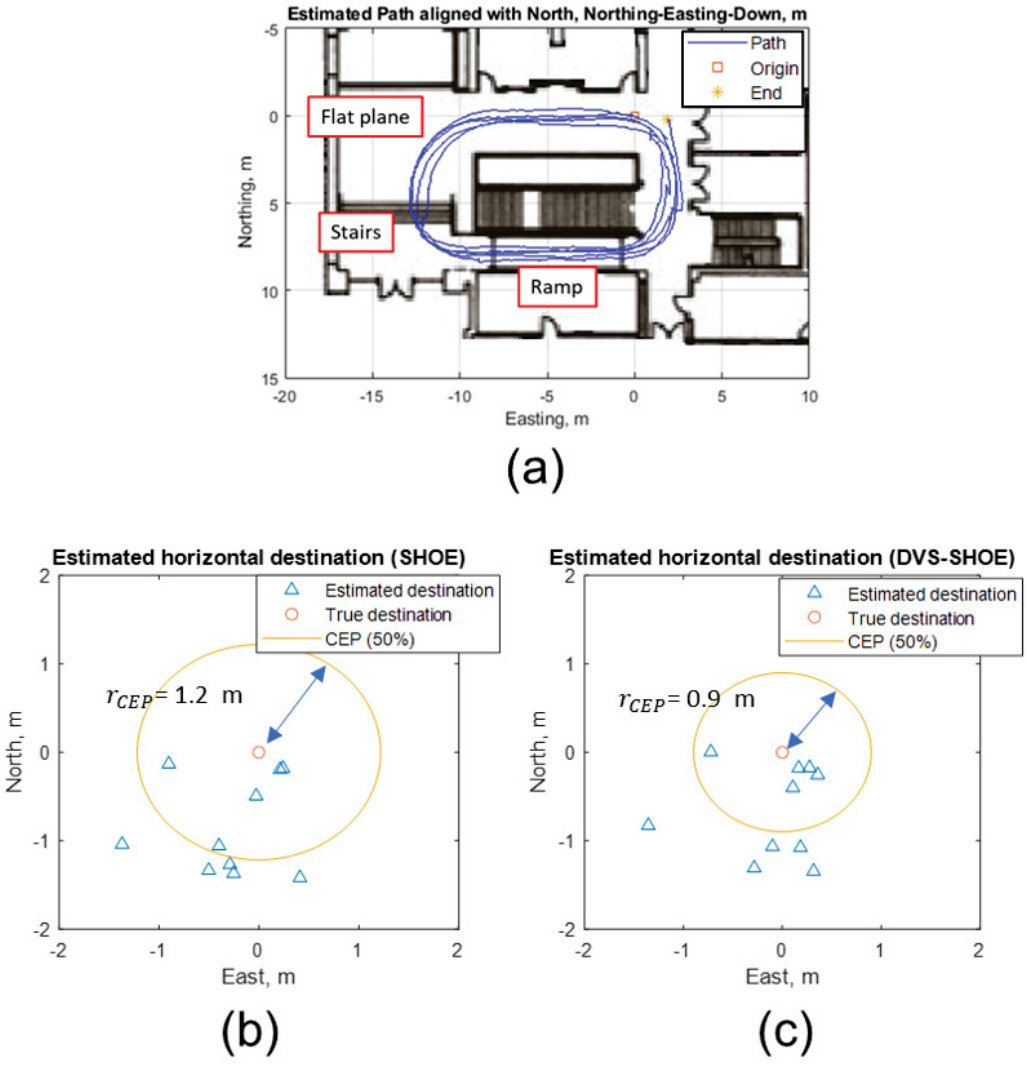

Figure 6. (a) Reference trajectory of the indoor walking experiments. (b) presents the navigation results of the SHOE detector in the indoor walking experiments. (c) demonstrates the navigation results of the DVS-SHOE detector in the indoor walking experiments.

improvement is a direct result of the fact that the DVS-SHOE detector has a better zero-velocity detection performance than the SHOE detector.

The DVS-SHOE detector has two constraints. First, we assumed that the scene observed by the DVS is static to use the DVS firing rate for zero-velocity detection. Nevertheless, this is not always the case. If the DVS observes moving objects during the stance phase, the statistics of the DVS-SHOE will increase, leading to mis-detections. Second, if the scene inside the field of view does not have many visual features, for example, a white wall, then the statistics of the DVS-SHOE will decrease, leading to false alarms.

6. Conclusion

In this paper, we proposed a novel zero velocity detector, the DVS-SHOE detector, for ZUPT-aided INS augmented by a foot-mounted event-based camera DVS128. We demonstrated that the firing rate of the foot-mounted DVS increased during the swing phase and decreased during the stance phase in a walking experiment. We experimentally determined the DVS mounting configuration, which is to mount the DVS next to an IMU and face the sensor outward for optimal performance of zero-velocity detection. We used two methods to evaluate the proposed DVS-SHOE detector. First, we compared the detection performances of the SHOE detector and the DVS-SHOE detector in terms of false alarm rate and detection rate. The experimental results showed that the DVS-SHOE detector achieved a lower false alarm rate than the SHOE detector. Second, we compared the navigation performance of the ZUPT-aided INS using the SHOE detector and the DVS detector. The experimental results showed that the CEP of the case using DVS-SHOE is reduced by around $25\,\%$, from $1.2\,m$ to $0.9\,m$, as compared to the case of the SHOE detector.

Acknowledgement

This work is performed under the following financial assistance award: 70NANB17H192 from US Department of Commerce, National Institute of Standards and Technology (NIST).

EN was supported by the National Science Foundation (NSF) under grant 1652159.

References

[1] C. Fischer and H. Gellersen, "Location and navigation support for emergency responders: A survey," *IEEE Pervasive Computing,* vol. 9, p. 38–47, 2010.

[2] Y. Chen, R. Chen, L. Pei, T. Kröger, H. Kuusniemi, J. Liu and W. Chen, "Knowledge-based error detection and correction method of a multi-sensor multi-network positioning platform for pedestrian indoor navigation," in *IEEE/ION Position, Location and Navigation Symposium*, Indian Wells, CA, USA, May 3-6, 2010.

[3] L. Chen, H. Kuusniemi, Y. Chen, L. Pei, T. Kröger and R. Chen, "Motion restricted information filter for indoor bluetooth positioning," *International Journal of Embedded and Real-Time Communication Systems (IJERTCS),* vol. 3, p. 54–66, 2012.

[4] A. Abdallah, K. Shamaei and Z. Kassas, "Indoor Localization with LTE Carrier Phase Measurements and Synthetic Aperture Antenna Array," in *ION GNSS*, Miami, FL, Sep. 16-20, 2019.

[5] D. B. Jourdan, D. Dardari and M. Z. Win, "Position error bound for UWB localization in dense cluttered environments," *IEEE Transactions on Aerospace and Electronic Systems,* vol. 44, p. 613–628, 2008.

[6] C. Keßler, C. Ascher, M. Flad and G. F. Trommer, "Multi-sensor indoor pedestrian navigation system with vision aiding," *Gyroscopy and Navigation,* vol. 3, p. 79–90, 2012.

[7] R. Jirawimut, S. Prakoonwit, F. Cecelja and W. Balachandran, "Visual odometer for pedestrian navigation," *IEEE Transactions on Instrumentation and Measurement,* vol. 52, p. 1166–1173, 2003.

[8] D. Titterton, J. L. Weston and J. Weston, Strapdown inertial navigation technology, vol. 17, IET, 2004.

[9] E. Foxlin, "Pedestrian tracking with shoe-mounted inertial sensors," *IEEE Computer Graphics and Applications,* p. 38–46, 2005.

[10] S. Godha and G. Lachapelle, "Foot mounted inertial system for pedestrian navigation," *Measurement Science and Technology,* vol. 19, p. 075202, 2008.

[11] Y. Wang, A. Chernyshoff and A. M. Shkel, "Error analysis of ZUPT-aided pedestrian inertial navigation," in *International Conference on Indoor Positioning and Indoor Navigation (IPIN)*, Nantes, France, Sep. 24-27, 2018.

[12] Y. Wang and A. M. Shkel, "A Review on ZUPT-Aided Pedestrian Inertial Navigation," in *27th Saint Petersburg International Conference on Integrated Navigation Systems (ICINS)*, Saint Petersburg, Russia, May 25-27, 2020.

[13] J.-O. Nilsson, A. K. Gupta and P. Händel, "Foot-mounted inertial navigation made easy," in *International Conference on Indoor Positioning and Indoor Navigation (IPIN)*, Busan, Korea, Oct. 27-30, 2014.

[14] Y. Wang, Y.-W. Lin, S. Askari, C.-S. Jao and A. M. Shkel, "Compensation of

Systematic Errors in ZUPT-Aided Pedestrian Inertial Navigation," in *IEEE/ION Position, Location and Navigation Symposium (PLANS)*, Portland, OR, Apr. 20-23, 2020.

[15] Y. Wang, S. Askari, C.-S. Jao and A. M. Shkel, "Directional ranging for enhanced performance of aided pedestrian inertial navigation," in *IEEE International Symposium on Inertial Sensors and Systems (INERTIAL)*, Naples, FL, Apr. 1-5, 2019.

[16] C.-S. Jao, Y. Wang and A. M. Shkel, "Pedestrian Inertial Navigation System Augmented by Vision-Based Foot-to-foot Relative Position Measurements," in *IEEE/ION Position, Location and Navigation Symposium (PLANS)*, Portland, OR, Apr. 20-23, 2020.

[17] C.-S. Jao, Y. Wang, S. Askari and A. M. Shkel, "A Closed-Form Analytical Estimation of Vertical Displacement Error in Pedestrian Navigation," in *IEEE/ION Position, Location and Navigation Symposium (PLANS)*, Portland, OR, Apr. 20-23, 2020.

[18] C.-S. Jao, Y. Wang, Y.-W. Lin and A. M. Shkel, "A Hybrid Barometric/Ultrasonic Altimeter for Aiding ZUPT-based Inertial Pedestrian Navigation Systems," in *ION GNSS*, Richmond Heights, Mo (virtual), Sep. 21-25, 2020.

[19] P. Robertson, M. Frassl, M. Angermann, M. Doniec, B. J. Julian, M. G. Puyol, M. Khider, M. Lichtenstern and L. Bruno, "Simultaneous localization and mapping for pedestrians using distortions of the local magnetic field intensity in large indoor environments," in *International Conference on Indoor Positioning and Indoor Navigation*, Montbeliard-Belfort, France, Oct. 28-31, 2013.

[20] M. Kok and A. Solin, "Scalable magnetic field SLAM in 3D using Gaussian process maps," in *21st International Conference on Information Fusion (FUSION)*, Cambridge, UK, Jul. 10-13, 2018.

[21] I. Skog, P. Handel, J.-O. Nilsson and J. Rantakokko, "Zero-velocity detection—An algorithm evaluation," *IEEE Transactions on Biomedical Engineering,* vol. 57, p. 2657–2666, 2010.

[22] R. Zhang, H. Yang, F. Höflinger and L. M. Reindl, "Adaptive zero velocity update based on velocity classification for pedestrian tracking," *IEEE Sensors Journal,* vol. 17, p. 2137–2145, 2017.

[23] M. S. Lee, C. Park and C. W. Shim, "A movement-classification algorithm for pedestrian using foot-mounted IMU," in *International Technical Meeting of The Institute of Navigation*, Newport Beach, CA, USA, Jan. 31-1, 2012.

[24] S. Y. Park, H. Ju and C. G. Park, "Stance phase detection of multiple actions for military drill using foot-mounted IMU," S*ensors,* vol. 14, p. 16, 2016.

[25] X. Tian, J. Chen, Y. Han, J. Shang and N. Li, "A novel zero velocity interval detection

algorithm for self-contained pedestrian navigation system with inertial sensors," *Sensors,* vol. 16, p. 1578, 2016.

[26] B. Wagstaff, V. Peretroukhin and J. Kelly, "Improving foot-mounted inertial navigation through real-time motion classification," in *International Conference on Indoor Positioning and Indoor Navigation (IPIN)*, Sapporo, Japan, Sep. 18-21, 2017.

[27] B. Wagstaff and J. Kelly, "LSTM-based zero-velocity detection for robust inertial navigation," in *International Conference on Indoor Positioning and Indoor Navigation (IPIN)*, Nantes, France, Sep. 24-27, 2018.

[28] Q. Wang, Z. Guo, Z. Sun, X. Cui and K. Liu, "Research on the forward and reverse calculation based on the adaptive zero-velocity interval adjustment for the foot-mounted inertial pedestrian-positioning system," *Sensors,* vol. 18, p. 1642, 2018.

[29] Y. Li and J. J. Wang, "A robust pedestrian navigation algorithm with low cost IMU," in *International Conference on Indoor Positioning and Indoor Navigation (IPIN)*, Sydney, Australia, Nov. 13-15, 2012.

[30] J. Wahlstrom, I. Skog, F. Gustafsson, A. Markham and N. Trigoni, "Zero-Velocity Detection-A Bayesian Approach to Adaptive Thresholding," *IEEE Sensors Letters,* 2019.

[31] Y. Wang and A. M. Shkel, "Adaptive threshold for zero-velocity detector in ZUPT-aided pedestrian inertial navigation," *IEEE Sensors Letters,* vol. 3, pp. 1-4, 2019.

[32] W. Sun, W. Ding, H. Yan and S. Duan, "Zero velocity interval detection based on a continuous hidden Markov model in micro inertial pedestrian navigation," *Measurement Science and Technology,* vol. 29, p. 065103, 2018.

[33] A. Norrdine, Z. Kasmi and J. Blankenbach, "Step detection for ZUPT-aided inertial pedestrian navigation system using foot-mounted permanent magnet," *IEEE Sensors Journal,* vol. 16, p. 6766–6773, 2016.

[34] Q. Wang, X. Zhang, X. Chen, R. Chen, W. Chen and Y. Chen, "A novel pedestrian dead reckoning algorithm using wearable EMG sensors to measure walking strides," in *Ubiquitous Positioning Indoor Navigation and Location Based Service*, Kirkkonummi, Finland, Oct. 14-15, 2010.

[35] M. Ma, Q. Song, Y. Gu, Y. Li and Z. Zhou, "An adaptive zero velocity detection algorithm based on multi-sensor fusion for a pedestrian navigation system," *Sensors,* vol. 18, p. 3261, 2018.

[36] C.-S. Jao, Y. Wang and A. M. Shkel, "A Zero Velocity Detector for Foot-mounted InertialNavigation Systems Aided by Downward-facing Range Sensor," in *IEEE Sensors Conference*, Rotterdam, Netherlands (virtual), Oct. 25-28, 2020.

[37] C. Zhou, J. Downey, D. Stancil and T. Mukherjee, "A low-power shoe-embedded radar for aiding pedestrian inertial navigation," *IEEE Transactions on Microwave Theory and Techniques,* vol. 58, p. 2521–2528, 2010.

[38] R. Zhang, F. Hoeflinger, O. Gorgis and L. M. Reindl, "Indoor localization using inertial sensors and ultrasonic rangefinder," in *International Conference on Wireless Communications and Signal Processing (WCSP)*, Nanjing, China, Nov. 9-11, 2011.

[39] P. Lichtsteiner, C. Posch and T. Delbruck, "A 128 × 128 120 dB 15 μs Latency Asynchronous Temporal Contrast Vision Sensor," *IEEE Journal of Solid-State Circuits,* vol. 43, p. 566–576, 2008.

[40] D. Weikersdorfer, D. B. Adrian, D. Cremers and J. Conradt, "Event-based 3D SLAM with a depth-augmented dynamic vision sensor," in *IEEE International Conference on Robotics and Automation (ICRA)*, Hong Kong, China, May 31-5, 2014.

[41] D. Weikersdorfer, R. Hoffmann and J. Conradt, "Simultaneous localization and mapping for event-based vision systems," in *International Conference on Computer Vision Systems*, St. Petersburg, Russia, Jul. 16-18, 2013.

[42] E. Mueggler, B. Huber and D. Scaramuzza, "Event-based, 6-DOF pose tracking for high-speed maneuvers," in *IEEE/RSJ International Conference on Intelligent Robots and Systems*, Chicago, Illinois, Sep. 14-18, 2014.

[43] G. Gallego, T. Delbruck, G. Orchard, C. Bartolozzi, B. Taba, A. Censi, S. Leutenegger, A. Davison, J. Conradt, K. Daniilidis and others, "Event-based vision: A survey," *arXiv preprint arXiv:1904.08405,* 2019.

[44] S. Askari, C.-S. Jao, Y. Wang and A. M. Shkel, "A Laboratory Testbed for Self-Contained Navigation," in *IEEE International Symposium on Inertial Sensors and Systems (INERTIAL)*, Naples, FL, Apr. 1-5, 2019.